



Research article

Heat transfer analysis: convective-radiative moving exponential porous fins with internal heat generation

Zia Ud Din¹, Amir Ali¹, Zareen A. Khan^{2,*} and Gul Zaman¹

¹ Department of Mathematics, University of Malakand Chakdara Dir(L), Khyber Pakhtunkhwa, Pakistan

² Department of Mathematical Sciences, College of Science, Princess Nourah bint Abdulrahman University, P.O. Box 84428, Riyadh 11671, Saudi Arabia

* **Correspondence:** Email: zakhan@pnu.edu.sa.

Abstract: The efficiency, temperature distribution, and temperature at the tip of straight rectangular, growing and decaying moving exponential fins are investigated in this article. The influence of internal heat generation, surface and surrounding temperatures, convection-conduction, Peclet number and radiation-conduction is studied numerically on the efficiency, temperature profile, and temperature at the tip of the fin. Differential transform method is used to investigate the problem. It is revealed that thermal and thermo-geometric characteristics have a significant impact on the performance, temperature distribution, and temperature of the fin's tip. The results show that the temperature distribution of decaying exponential and rectangular fins is approximately 15 and 7% higher than growing exponential and rectangular fins respectively. It is estimated that the temperature distribution of the fin increases by approximately 6% when the porosity parameter is increased from 0.1 to 0.5. It is also observed that the decay exponential fin has better efficiency compared to growing exponential fin which offers significant advantages in mechanical engineering.

Keywords: convection; convective boundary conditions; exponential porous fins; mathematical model; radiation

1. Introduction

There have been many systems designed, ranging from tiny electronic devices to massive industrial machinery. During operation of these systems, heat is generated. For the system to function properly, improving the geometry is vital to increase heat transfer and prevent heat loss. In this study, we investigate which fin geometry is more efficient and easy to install.

The introduction of new technologies has received considerable attention in order to enhance the

NOMENCLATURE

h	Convection heat transfer coefficient ($W/m^2 K$)	A	Area of fin's surface (m^2)
W	width of the fin (m)	P	fin's perimeter (m)
U	Speed of moving fin (m/s)	N	Dimensionless convection parameter
x	Direction along x-axis (m)	X	Dimensionless coordinate
g	Gravitational acceleration (m/s^2)	L	Fins length (m)
q	Internal heat generation (W)	T	Dimensional fin temperature (K)
K	Porous fins permeability (m^2)	R_a	Rayleigh number ($g\beta t^3(T_b - T_a)/\lambda\nu$)
Q	Dimensionless internal heat generation/absorption parameter	K_s	Solid thermal conductivity ($W/m K$)
k_r	Ratio of thermal conductivity (k_{eff}/k_s)	P_e	Peclet number, dimensionless
T_a	Ambient temperature (K)	k_{eff}	Effective thermal conductivity ($W/m K$)
T_s	Dimensional surface temperature (K)	k_f	Air thermal conductivity ($W/m K$)
T_b	Base temperature (K)	S_g	Porosity parameter
C_p	Specific heat of the material (J/kgK)	N_r	Dimensionless radiation parameter
D_a	Darcy number (K/t^2)	\dot{m}	Mass flow rate (kg/s)
Greek letters			
λ	Thermal diffusivity of air (m^2/s)	β	Volume expansion coefficient (K^{-1})
θ	Dimensionless local temperature	ν	Kinematic viscosity of air (m^2/s)
ε	Surface emissivity	ρ	density of material (kg/m^3)
α^*	Dimensionless fin shape parameter	α	Fin shape parameter
η	Fin efficiency	σ	Stefane-Boltzmann constant ($W/m^2 K^4$)
φ	Porosity of the fin	τ_b	Thickness of the fin (m)
θ_a	Dimensionless ambient temperature	θ_s	Dimensionless surface temperature
θ_b	Dimensionless base temperature		

efficiency of heat transfer from various heating systems such as automobiles, power plants, diesel engines, geothermal energy and other industrialized heat-generating systems. According to researchers even with modern engine technologies, 30–40% of the energy is still misspend through the exhaust system and approximately 15–30% of the energy is converted to useful works [1]. However, it is observed that the production of internal combustion engines (ICEs) is rapidly increasing, raising concerns about the potential for an increase in dangerous greenhouse gases (GHG). As a result, scientists are motivated to use methods to recycle heat from waste sources in engines, which often decreases the need for energy production, but also reduces GHG emissions and improvements in energy efficiency [2]. However, because the exhaust heat exchanger can produce a pressure loss and affect engine output, its design plays an imperative role. To choose an effective heat exchanger design, first, consider the limitations of each heat exchanger model. Although costs of production are the most significant factor, temperature ranges, thermal efficiency, pressure limits, fluid flow capability, pressure drop, maintenance, clean-ability, materials, and so on are also significant. The use of fins is one of the most efficient methods for transferring heat [3]. Therefore, scientists and engineers are searching for more effective and economical means to enhance the amount of heat transfer while cooling down the equipment of current advancement [4].

Fins are one of the most effective tools to optimize cost and space in modern technology. A fin is an enlarged surface that is designed to promote heat transmission from a warm surface to the surrounding fluid. Fins are primarily used to increase the heat exchange rate. Fins are also extensively used in the cooling of pipelines carrying oil that are hundreds of miles long. Furthermore, electronic chips cannot work properly without fins to dissipate heat. The fin's heat transfer mechanism is to transfer heat from its base to its surface and then transfer this heat through radiation and convection to the surrounding medium. In addition to conventional applications of heat transfer such as internal combustion engines, heat evaporators, and compressors, fins are also powerful tools used in space vehicles, computer processor cooling, and other electronic components for heat dissipation [5]. The car radiator, refrigerator compressor, and air conditioner radiators are the most common applications of fins surfaces [6].

A moving type of exponential fin is studied here, along with heat generation and absorption sources. By the moving fin, we mean that the heat transfer from the hot exterior to the ambient medium occurs in continuous motion. Currently, the study of heat transfer from fins reveals that moving exponential fins of various geometries are essential when these fins are available to a heat-generating medium [7,8]. There are several industrial processes, such as glass fiber drawing, extrusion, casting, and hot rolling, which was modelled on the moving fins [9].

Several studies have been performed to analyze heat transfer from exponential fin and observed that growing exponential fin is more efficient than rectangular fin [10–12]. Numerical investigation of conjugate heat dissipation in a double-tube using DGFEM with fins of the exponential profile was performed and observed that efficiency of the exponential fin is higher up to 15% than triangular fin [13]. Temperature distribution of circular convective fins of different profiles is studied using the least square method (LSM) [3]. The Differential transform method (DTM) has been applied to analyze exponential fin [14, 15].

Fins phenomena and their interesting features can be studied using a variety of mathematical techniques, such as integral equation method [16], Homotopy perturbation [17], Homotopy analysis [18], and Adomian decomposition method (ADM) [19]. These methods are used to exchange heat from a convective-conductive and radiative moving fin as well as a convective-radiative fin with variable thermal conductivity. A uni-dimensional convective-radiative fin having temperature-dependent conductivity was analysed by [20]. They developed a novel approach for transforming the nonlinear ODEs into an algebraic equation using the first-order Taylor's expansion. The heat transfer rate and fin performance of a straight fin having variable convective heat transfer coefficient and thermal conductivity were calculated analytically by [21]. Similarly, analytic solutions for rectangular straight fins were obtained to study the efficiency and technique of mass transfer in terms of heat transfer [22]. The heat transfer performance in the finned heat pipe framework used in the central processing unit (CPU) has also been studied [23]. It has been concluded that the ideal direction for cooling the pipe system letting to remove maximum heat is the thermo-siphon position that allows eliminating heat as high as 150W if one considers that the CPU works securely with a constant temperature lower than 90C°.

The effect of thermal conductivity and thermo-geometric parameters on the productivity and efficiency of straight convective fins has been investigated in [24]. A fin cluster in radiation-conduction in a non-active source or the mechanics of heat exchange in one-dimensional transmitting fins and space radiators are examined in a broad manner [25, 26]. Using the surface temperature response in a radial porous fin, an inverse methodology is used to study both internal heat generation and magnetic field strength at the same time [27, 28]. Heat exchange from a T shape porous fin was analyzed by [29]

applying Adomian decomposition method and observed that heat transfer increases by increasing the base temperature while increasing the surrounding temperature show reverse effect. The performance and design of porous fin have been studied by [30,31] an effort has been made to construct an analytic model for evaluating the effectiveness and optimal dimensions of porous fins while taking into account various prediction models. Every finding has been described in a comparable manner so that the worth of the models may be easily recognized. A cylindrical porous fin is studied by using Runge-Kutta method and inverse, and an inverse problem is solved for estimating unknown parameters. It is found that the hybrid method performs better and yields relatively faster convergence than the individual methods [32, 33]. Recently [34] analyzed the porous radial, spin and longitudinal fin with multiple nonlinearities and compared the analysis of the porous fin with the solid fin. And concluded that, depending on the value of the porosity and natural convection involved in designing the porous fin, it can perform better than the solid fin. In a similar manner, the entropy generation in the convective porous fin of rectangular profile as well as a minimum shape of the porous fin with temperature-dependent thermal conductivity have been analyzed analytically [35, 36]. As a result, the enactment of the fin increases with radiation. Based on the analytical study, it was determined that the highest efficiency can be achieved by using an exponential fin geometry that plays a critical role in enhancing heat transfer [37–39].

The distribution of temperature in a porous fin material, that is, Aluminum (*Al*) and Silicon nitride (Si_3N_4) were studied numerically by considering temperature depending on heat generation [40]. It was assumed that fins made of porous aluminum transmit more heat than the Silicon nitride (Si_3N_4) compound. Similarly, the practical uses of porous fins to improve refrigeration efficiency have been explored for the micro-tube heat sink, and for ceramic-based materials [41]. Furthermore, a wet loading condition was presented to execute effective heat exchange over the fins of an exponential profile [42]. Exponential fins systems are designed and analyzed mathematically by [43] and concluded that the thermal competence of the exponential fin is lower than those of parabolic and triangular fins. Moreover, it is observed that exponential fins may transmit more heat than the fin of rectangular profiles. Heat exchange between a moving exponential fin exposed to heat has been studied analytically [44–46]. A heat exchanger with curved rectangular fins is investigated for its convection heat transfer in turbulent flow by [47] and concluded that a double phase heat exchanger without a fin has a heat transfer coefficient 81% lower than one with a rectangular fin. An effective thermal conductivity model is used to analyze the microstructure and inertial characteristics of Ferro fluid over a stretching sheet [48, 49]. Electro-osmotic flow in a nanochannel via semi analytical method is solved by using (HPM) and concluded that the (HPM) is accurate, reliable and easy to use [50].

According to [51], exponential fins can replace conventional rectangular fins for improved heat transfer rates and better fin efficiency in industrial applications compared to straight rectangular fins commonly used. In light of this perspective, it is imperative to investigate the combined impact of motion of the fin, loss of heat through convection and radiation, heat generation/absorption by deriving the associated governing heat equation, and to study the analytical as well as the numerical solutions with the supposition of constant heat transfer coefficient h and constant thermo-physical behaviour.

Problem statement

We study temperature distribution, the temperature at the fin's tip and the efficiency of exponential fins. In this study, both numerical and semi-analytical methods are used to investigate the heat transfer.

Various types of exponential fins for convection-conduction number, radiation-conduction number, ambient and surface temperatures, Peclet number and internal heat are compared.

2. Problem description

Here, we consider the heat exchange in the longitudinal exponential fins of length L together with both convection and radiation parameters. The physical parameters involved in the model are S_g porosity, h heat transfer coefficient, T_a ambient temperature, T_b temperature of the fin base, T_s the surface temperature, ρ density of the fin material, h heat transfer coefficient, T temperature distribution. The specific heat of the exponential fin is C_p , the emissivity of the material is ε , and the Stefan-Boltzmann constant is Σ . It should be noted that the thermal conductivity k and heat transfer coefficient h of the fin are considered to be fixed. The convection heat transfer coefficient h is constant and uniform over the entire surface of the fin for convenience in the analysis. A moving fin emits radiation only from its surface, with no visible absorption of radiation from its surroundings; therefore, its thermal emissivity is considered to be constant.

- 1) Porous fins are assumed to have a steady state heat transfer.
- 2) It is assumed that the fin's thickness is significantly smaller than all other dimensions, so the temperature is significantly affected only in the longitudinal direction.
- 3) Fluid is assumed to be homogeneous, isotropic and single phase in porous media.
- 4) It is assumed that Darcy's law governs fluid-solid interactions.
- 5) A uniform temperature is maintained at the fin's base without any contact resistance.
- 6) Fluids and solids are in thermal equilibrium locally.

Let us consider that the fin is moving at a velocity U . This means that the heat loss from the hot surface to the adjacent fluid occurs in continuous motion, and x is the distance from the fin's base. The governing equation has been extensively studied before for straight porous fins after an energy balance. The local formation of the fin having exponential geometry can be represented by [52]

$$f(x) = \tau_b e^{\alpha^* x}, \quad (2.1)$$

where α^* is dimensional shape parameter of fin [39] and τ_b is semi-fin thickness. Without loss of generality, the thickness at the base of fin is fixed to 1. Although the results are for this specific fin thickness at the base of fin base, it should be noticed that by allowing for variable thickness, an optimum thickness can be achieved. It is discovered that $\alpha^* = 0$ represents a straight rectangular fin, but $|\alpha^*| > 0$ represents a growing and decaying type of exponential fin as shown in Figure 1. The governing equation of the moving fin with exponential shape together with heat generation source, porous parameter, and heat exchange through radiation and convection is given by [51]

$$\frac{d}{dx} \left[f(x) \frac{dT}{dx} \right] + \left[\frac{U (\rho C_p)_{eff} dT}{k_{eff}} + \frac{q}{k_{eff}} \right] f(x) - \frac{h(1-\varphi)P}{A k_{eff}} [T - T_a] - \dot{m} C_p [T - T_a] - \frac{\varepsilon \sigma P}{A k_{eff}} [T^4 - T_s^4] = 0. \quad (2.2)$$

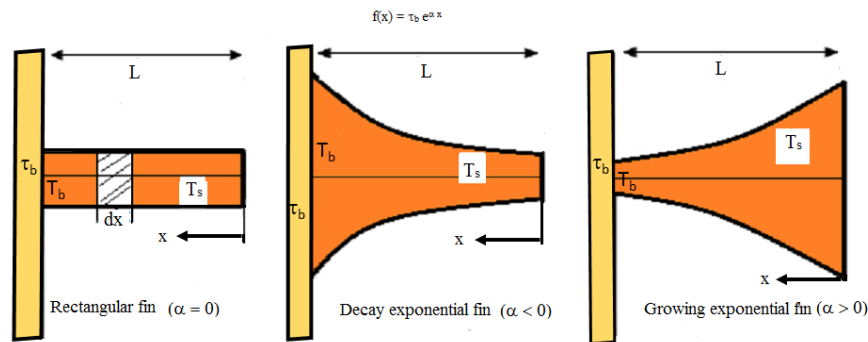


Figure 1. Schematic diagram of rectangular fin, decay and growing exponential fin.

The mass flow rate \dot{m} of the air flowing through the porous medium is represented by

$$\dot{m} = \rho v_w \varphi W \Delta x, \quad (2.3)$$

where φ represent porosity of the fin. the value of φ ranges from 0 to 1 for a solid medium $\varphi = 0$ and if $\varphi = 1$ there will be no solid portion. V_w represent the Darcy formula defined as [53]

$$v_w = \frac{\beta g K}{\nu} [T - T_a]. \quad (2.4)$$

The enthalpy flux In case of porous materials can be stated as $(\rho C_p)_{eff} U \frac{dT}{dx}$ [34] where

$$(\rho C_p)_{eff} = (1 - \varphi) \rho_s C_{ps} + \varphi \rho_f C_{pf}. \quad (2.5)$$

We further define an effective thermal conductivity

$$k_{eff} = \varphi k_f + [1 - \varphi] k_s. \quad (2.6)$$

Here k_{eff} represent effective thermal conductivity and φ fin's porosity. Using Eqs (2.3)–(2.6), and simplifying, Eq (2.2) we obtain

$$\begin{aligned} \frac{d}{dx} \left[f(x) \frac{dT}{dx} \right] + \left[\frac{U}{\lambda} \frac{dT}{dx} + \frac{q}{k_{eff}} \right] f(x) - \frac{h(1-\varphi)P}{A k_{eff}} [T - T_a] - \frac{\rho \beta g C_p K \varphi W}{\nu k_{eff}} [T - T_a]^2 \\ - \frac{\varepsilon \sigma P}{A k_{eff}} [T^4 - T_s^4] = 0, \end{aligned} \quad (2.7)$$

where $\lambda = k_{eff}/(\rho C_p)_{eff}$ is thermal diffusivity of the fin's material. To non-dimensionalize the above equation, we consider

$$\begin{aligned} \alpha^* = \frac{\alpha}{L}, \quad X = \frac{x}{L}, \quad \theta = \frac{T}{T_b}, \quad \theta_a = \frac{T_a}{T_b}, \quad \theta_s = \frac{T_s}{T_b}, \quad S_g = \frac{D_a R_a (L/t)^2}{k_r}, \quad D_a = \frac{\varphi K}{t^2}, \\ R_a = \frac{g \beta t^3 [T_b - T_a]}{\lambda \nu}, \quad P_e = \frac{UL}{\lambda}, \quad Q = \frac{qL^2}{T_b k_{eff}}, \quad N_r = \frac{\varepsilon \sigma P L^2 T_b^3}{A k_{eff}}, \quad N^2 = \frac{h(1-\varphi) P L^2}{A k_{eff}}. \end{aligned}$$

After simplification, Eq (2.7) gives

$$e^{\alpha X} \frac{d^2 \theta}{dX^2} + e^{\alpha X} [\alpha + Pe] \frac{d\theta}{dX} - N^2 [\theta - \theta_a] - S_g [\theta - \theta_a]^2 + Q e^{\alpha X} - N_r [\theta^4 - \theta_s^4] = 0, \quad (2.8)$$

which demonstrate that distribution of temperature of the fin depends on Peclet number, Pe , convection-conduction parameter, N , temperature ratios, θ_a and θ_s , radiation-conduction parameter N_r , Porosity parameter S_g , and interior heat absorption/generation parameter Q . Rearranging the above equation, we obtain

$$e^{\alpha X} \frac{d^2 \theta}{dX^2} + A e^{\alpha X} \frac{d\theta}{dX} - B \theta - S_g \theta^2 - N_r \theta^4 + C + Q e^{\alpha X} = 0, \quad (2.9)$$

where

$$A = 2\alpha - Pe, \quad B = N^2 - 2S_g \theta_a, \quad C = N^2 \theta_a + N_r \theta_s^4 - S_g \theta_a^2.$$

We will study fins with adiabatic boundary conditions. Most of the time, in practice, the fin tip is thin enough that the rear-end heat transfer can be neglected, and a solution can be obtained by assuming the fin tip is insulated. We consider that at base ($X = 1$) the fin's temperature is T_b . By adiabatic boundary condition, we mean that no heat transfer from the tip of the fin.

$$T \Big|_{x=L} = T_b, \quad \text{and} \quad \frac{dT}{dx} \Big|_{x=0} = 0.$$

By making dimensionless the boundary conditions, we obtain

$$\theta(1) = 1, \quad \frac{d\theta}{dX} \Big|_{X=0} = 0. \quad (2.10)$$

The efficiency η of the fin is the ratio of the total heat transfer from a fin to its utmost heat exchange if the whole fin is placed at equal temperature as its base temperature. For an exponential fin's efficiency is defined as [54]

$$\eta = \frac{\int_0^1 \left[N(\theta - \theta_a) + S_g(\theta - \theta_a)^2 + N_r(\theta^4 - \theta_s^4) \right] dX}{N_c(1 - \theta_a) + S_g(1 - \theta_a)^2 + N_r(1 - \theta_s^4)}. \quad (2.11)$$

3. Mathematical formulation

In this section, we use differential Transform Method (DTM) to calculate analytically Eq (2). The DTM is a semi-analytic technique based on Taylor expansion. Here, we use the proposed technique to calculate the analytical solution of the considered model. By using the DTM technique, it should be noted that the considered problem is transformed into algebraic equations and then coefficients are calculated. The differential transform method (DTM) exhibits the advantage of being able to solve nonlinear differential equations directly, eliminating the need to linearize or discretize. Let $\theta(y)$ be

analytic at a domain D , and let $y = y_0$ symbolize any point in D . The function $\theta(y)$ can be represented as a power series whose centre is located at y_0

$$\phi(k) = \frac{1}{k!} \left[\frac{d^k}{dx^k} \theta(y) \right]_{y=y_0}, \quad (3.1)$$

where $\phi(k)$ for $k \in Z^+$ is a transformed function while $\theta(x)$ is primary function. The inverse differential transformation of $\phi(k)$ can be defined as

$$\theta(y) = \sum_{k=0}^{\infty} (y - y_0)^k \phi(k). \quad (3.2)$$

By combining Eqs (3.1) and (3.2), we obtain

$$\theta(y) = \sum_{k=0}^{\infty} (y - y_0)^k \frac{1}{k!} \left[\frac{d^k}{dx^k} \phi(k) \right]_{x=x_0}, \quad (3.3)$$

which is Taylor series expansion of $\theta(y)$ at $y = y_0$. Mathematical operation executed by DTM are presented in Table 1 The value of the function $\phi(k)$ for different values of k are discrete. Applying

Table 1. The fundamental concept of DTM.

S.No	regional function	Transformed function
1	$\theta(y) = \alpha f(t) \pm \beta g(t)$	$\phi(k) = \alpha F(k) \pm \beta G(k)$
2	$\theta(y) = \frac{df(t)}{dt}$	$\phi(k) = (k + 1)F(k + 1)$
3	$\theta(y) = \frac{d^2 f(t)}{dt^2}$	$\phi(k) = (k + 2)(k + 1)F(k + 2)$
4	$\theta(y) = e^{\gamma t}$	$\phi(k) = \frac{\gamma^k}{k!}$
5	$\theta(y) = f(t) g(t)$	$\phi(k) = \sum_{j=0}^k F(j)G(k - j)$
6	$\theta(y) = f(t) g(t) h(t)$	$\phi(k) = \sum_{l=0}^k \sum_{j=0}^l [F(j) G(l - j) H(k - l)]$
7	$\theta(y) = t^n$	$\phi(k) = \delta(k - n)$

DTM to Eq (2), we obtain

$$\begin{aligned} & \sum_{j=0}^k \frac{\alpha^j}{j!} (k - j + 1)(k - j + 2)\phi(k - j + 2) + A \sum_{j=0}^k \frac{\alpha^j}{j!} (k - j + 1)\phi(k - j + 1) - B \phi(k) \\ & - S_g \sum_{j=0}^k [\phi(j) \phi(k - j)] - N_r \sum_{l=0}^m \sum_{k=0}^l \sum_{j=0}^k \phi(j)\phi(k - j)\phi(l - k)\phi(m - l) \\ & + Q \cdot \frac{\alpha^k}{k!} + C \cdot \delta(k - 0) = 0. \end{aligned} \quad (3.4)$$

Here $\delta(k - n)$ is Dirac delta function define as

$$\delta(k - n) = \begin{cases} 0, & k \neq n, \\ 1, & k = n. \end{cases} \quad (3.5)$$

Applying the differential transformation on the boundary conditions given in Eq (2.10) at $X = 0$, we considers

$$\phi(1) = 0.0, \quad \phi(0) = a, \quad (3.6)$$

where a is a constant and will be determine in light of the second boundary condition in Eq (2.10). Further, solving Eq (3.4) for different value of k , we obtain

$$\begin{aligned} \phi(2) &= \frac{1}{2} (N_r a^4 + S_g a^2 + B a - A + C - Q), \\ \phi(3) &= \frac{1}{3} \left[-A \phi(2) + \frac{1}{2} B (-a\alpha + 1) + \frac{1}{2} a S_g (-a\alpha + 1) + \frac{1}{2} a^3 N_r (-a\alpha + 4) - \frac{1}{2} \alpha C \right], \\ \phi(4) &= -\frac{1}{4} A \phi(3) + \frac{1}{12} B \left[\phi(2) - \alpha + \frac{1}{2} \alpha^2 a \right] + \frac{1}{12} S_g \left[2a \phi(2) - 2a\alpha + 1 + 2\alpha^2 a^2 \right] \\ &\quad + \frac{1}{12} N_r \left[4a^3 \phi(2) - 4\alpha a^3 + 6a^2 + \frac{1}{2} \alpha^2 a^4 \right] + \frac{1}{24} C \alpha^2, \\ \phi(5) &= -\frac{1}{5} A \phi(4) + \frac{1}{20} B \left[\phi(3) - \alpha \phi(2) - \frac{1}{2} \alpha^2 - \frac{1}{6} \alpha^3 a \right] \\ &\quad + \frac{1}{20} S_g \left[2a \phi(3) - 2\phi(2) - 2\alpha a \phi(2) - \alpha + \alpha^2 a - \frac{1}{6} a^2 \alpha^3 \right] \\ &\quad + \frac{1}{20} N_r \left[4a^3 \phi(3) + 12a^2 \phi(2) - 4\alpha a^3 \phi(2) - 6\alpha a^2 + 4a + 2\alpha^2 a^3 - \frac{1}{6} a^4 \alpha^3 \right] - \frac{1}{120} C \alpha^3. \end{aligned}$$

Other terms can be calculated in the similar way. The final solution can be presented in the form of algebraic equation as

$$\theta(X) = a + \sum_{i=1}^{\infty} \phi(i) X^i. \quad (3.7)$$

To calculate the value of a , we put the the second boundary condition from Eq (2.10) in Eq (3.7) which gives

$$\theta(1) = a + \sum_{i=1}^{\infty} \phi(i) = 1. \quad (3.8)$$

The final solution is presented in Taylor series form as

$$\theta(x) = 0.6128 + 0.2X + \phi(2)X^2 + \phi(3)X^3 + \phi(4)X^4 + \phi(5)X^5 + \phi(6)X^6 + \phi(7)X^7 + \phi(8)X^8 + \dots \quad (3.9)$$

Table 2. The error analysis between the numerical and DTM solutions.

x	Numerical	DTM	Numerical-DTM	x	Numerical	DTM	Numerical-DTM
0	0.61240	0.61379	0.0014	0.1	0.63298	0.63673	0.0038
0.2	0.65501	0.66239	0.0074	0.3	0.67905	0.6903	0.0112
0.4	0.70577	0.71906	0.0133	0.5	0.73608	0.75211	0.0160
0.6	0.77115	0.78855	0.0174	0.7	0.81252	0.83095	0.0184
0.8	0.87805	0.87820	1.5×10^{-4}	0.9	0.93454	0.93498	4.4×10^{-4}

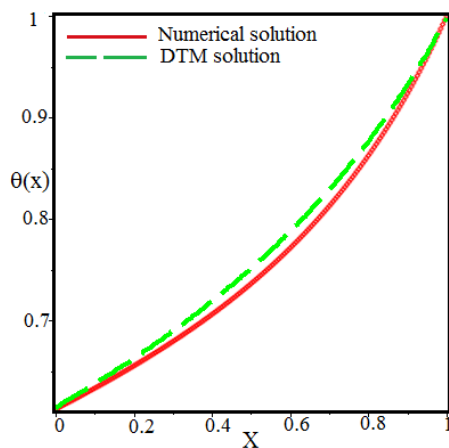


Figure 2. Comparison between the numerical solution of the governing model and the analytical approximation obtained by using DTM method for decay exponential porous fin for $N = 0.5, S_g = 0.5, \theta_s = 0.4, \theta_a = Pe = Q = N_r = 0.2$.

In the case of decay exponential fin the result of numerical solution and differential transform solution are compared. From Figure 2, one can see that the numerical solution and an approximation obtained by DTM gives a good agreement.

4. Results and discussion

In this section, we study the heat transfer from the moving exponential fins numerically, where convective and radiation heat exchange parameters along with porosity and thermal conductivity are considered. The dimensionless temperature distribution drop-down over the length of a fin is discussed for a variety of values.

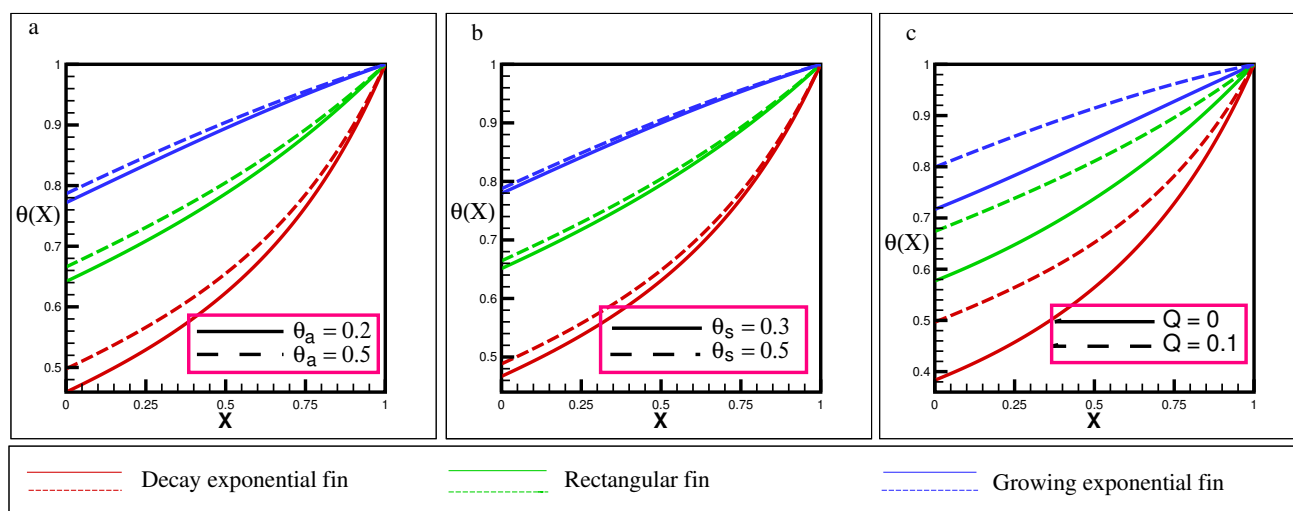


Figure 3. The above figures show the temperature distribution for a variety of fins under (a) The effect of internal heat generation Q , with $\theta_a = 0.2, \theta_s = 0.4$. (b) The effect of θ_a , with $Q = 0.2, \theta_s = 0.4$. (c) The effect of θ_s , with $Q = \theta_a = 0.2$. The values of other parameters are given as $N = 0.5, S_g = 0.5, Pe = N_r = 0.2$.

In Figure 3(a),(b), one can see that, with the enhancement of ambient and surface temperatures, the rate of temperature distribution decreases. Actually, as θ_a and θ_s grows, the convective heat dispersal from the surface of the moving fin decreases and thereby holds higher temperatures at the fin's exterior. The effect of heat generation Q , internally in the fins on the temperature distribution is given in Figure 3(c), which show that by increasing the internal heat generation parameter the temperature distribution increases as the temperature difference between the fin and the surrounding fluid increases. It should be noted that other parameters are kept invariant as mentioned in the caption of Figure 3. In conclusion, from Figure 3, we discovered that the temperature enhances rapidly when enhancing the value of internal heat generation Q , surrounding temperature θ_a and surface temperature θ_s .

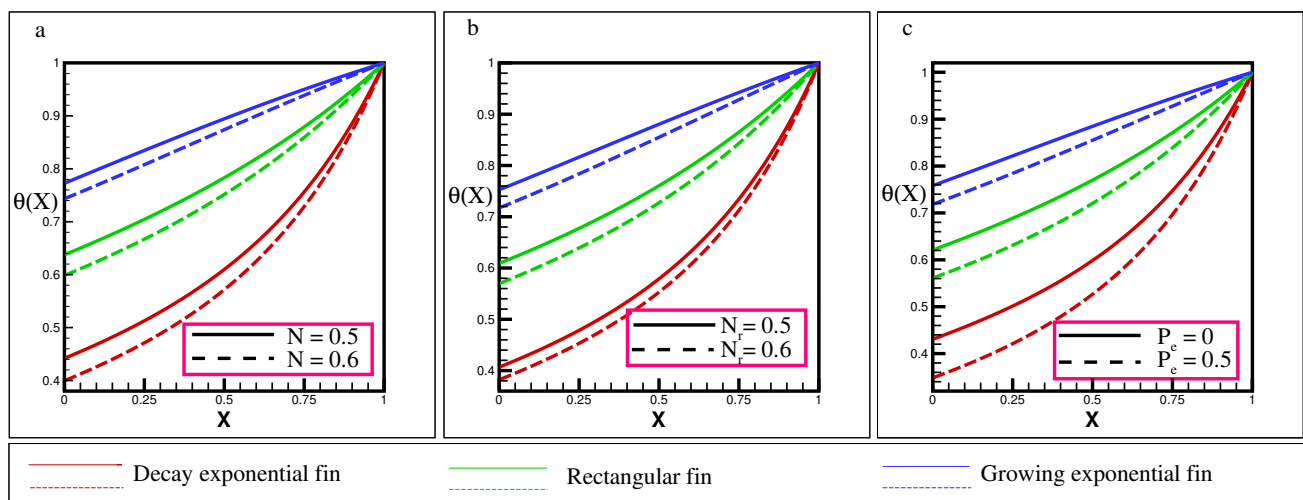


Figure 4. Comparison of temperature distribution for a variety of fins under (a) The effects of Thermo-geometric parameter N with $Pe = 0.2, N_r = 0.2$. (b) The effect of Thermo-geometric parameter N_r with $Pe = 0.2, N = 0.5$. (c) The effects of Peclet number Pe with $N = 0.5, N_r = 0.2$. The other parameters are considered as $S_g = 0.5, Q = \theta_a = 0.2, \theta_s = 0.4$.

In Figure 4(a),(b), the influence of increasing the convection-conduction number N and radiation-conduction number N_r are studied. Since N is the convection-to-conduction ratio, a rise in N indicates that more heat is transferred by convection, while less is transferred by conduction. The cooling process increases by 15% when N is increased from 0.5 to 0.6. There is a significant temperature drop along the rod by 5% due to the dissipated heat of the hot fin rising from 0.1 to 0.5. The influence of Pe on temperature profile is presented in Figure 4(c), which demonstrate the drop of temperature by rising the value of Pe . As the value of Pe rises the time for which the material is uncovered to the atmosphere gets shorter as well as the losing heat form fin exterior increases, causing the fin temperature to fall. When $Pe = 0$, indicating a static fin, cooling takes longer, as demonstrated by higher temperatures, when compared to a moving fin. Consequently, where cooling is required, a larger Peclet number is preferable.

From the results, it is deduced that the ratio of convection to conduction heat transfer coefficient has an incredible impact on fin's efficiency, temperature distribution and the rate of heat exchange at the fin's base.

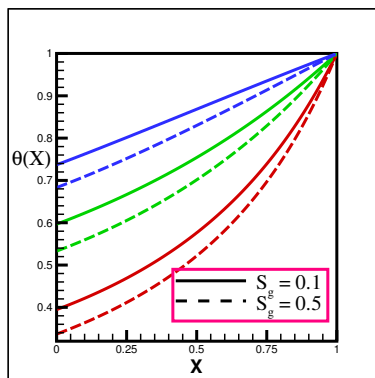


Figure 5. The effect of porosity parameter S_g on temperature distribution for $N = 0.5, \theta_a = 0.2, \theta_s = 0.4, Q = Pe = N_r = 0.2$.

In Figure 5, we present the influence of porosity parameter on temperature distribution. The temperature of the fin drop-down is observed with the enhancement in the porosity parameter. It is estimated that the temperature distribution of the fin increases by approximately 6% when the porosity parameter is increased from 0.1 to 0.5. A larger porosity parameter enhances the permeability of the porous fin as a result a higher temperature transfer occurs due to which temperature along with the fin surface decrease. Moreover, it is observed that in all the cases the temperature distribution from the growing exponential is lower than the rectangular fin which is lower than the decay exponential fin.

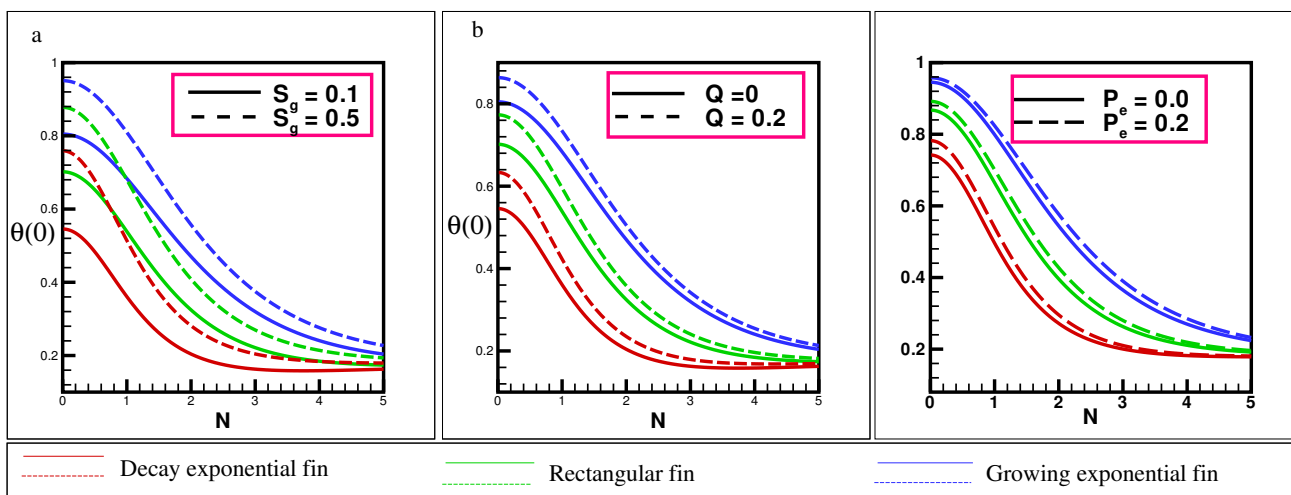


Figure 6. Comparison of fin’s tip temperature for a variety of fins against the convection-conduction number (a) The effects of porosity parameter for $Pe = 0.2, Q = 0.2$. (b) The effects of internal heat generation for $S_g = 0.5, Pe = 0.2$ (c) The effects of Peclet number for $S_g = 0.5, Q = 0.2$. The other parameter are considered as $N_r = \theta_a = 0.2, \theta_s = 0.4$.

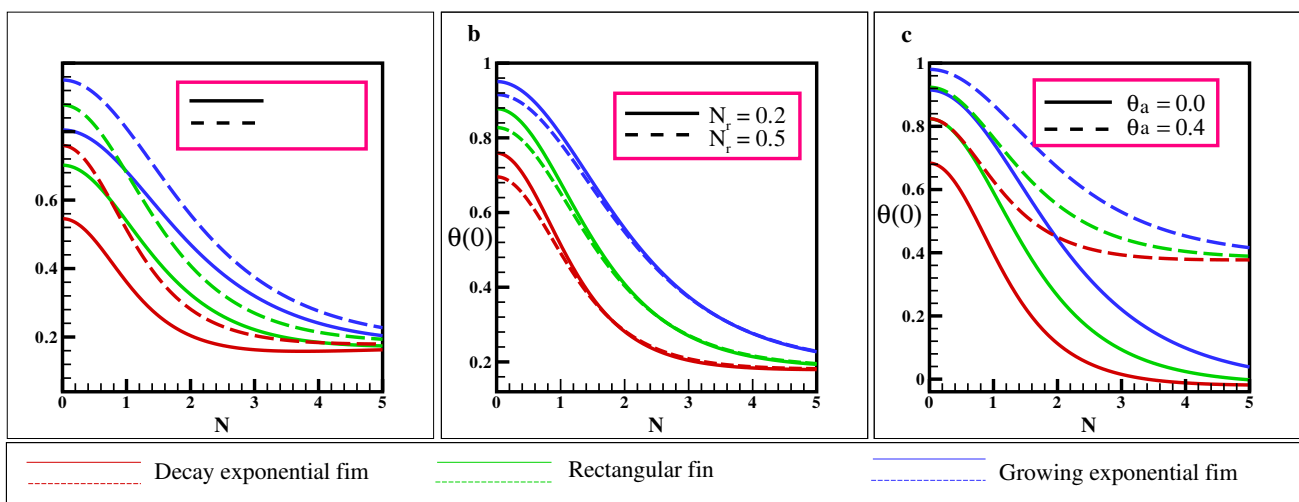


Figure 7. Comparison of fin's tip temperature for a variety of fins against the convection-conduction number (a) The effects of surface temperature for $N_r = 0.2, \theta_a = 0.2$. (b) The effects of radiation conduction number for $\theta_a = 0.2, \theta_s = 0.4$. (c) The effects of ambient temperature for $N_r = 0.2, \theta_s = 0.4$. The other parameters are considered as $S_g = 0.5, Q = Pe = 0.2$.

In Figures 6 and 7, we study the connection of the temperature distribution of the fin's tip against convection-conduction parameter N . The effect of porosity parameter S_g along with the convection-conduction parameter N on the temperature of the tip of the fin is represented in Figure 6(a). From this figure, one can see that, when N approaches zero, the temperature on the fin's tip decreases by increasing the value of porosity parameter S_g . But, when the value of N increases, the effect of the S_g on the tip temperature decreases. The effect of an internal heat generation is given in Figure 6(b). It should be noted that as Q increases from 0 to 0.2 we obtain the maximum value of the temperature for the minimum N on the fin's tip and the differences of the fin tip temperature decreases as N increases. The influence of Pe on fin's tip temperature is expressed in Figure 6(c). When the value of the Peclet number is small enough, that is, $Pe = 0$, the fin's tip temperature is increasing at a small value of N , relative to the larger value of the Peclet number while the influence of Pe on the temperature of the fin's tip declines with the increase of thermo-geometric parameter.

In Figure 7(a), we see that the temperature of the fin's tip decreases as the significance of surface temperature increases for a small value of N (convection-conduction number) and become closer to each other as N increases. Similarly, Figure 7(b), shows that at a small value of convection-conduction number N , the fin's tip temperature decreases as we increase radiation-conduction number N_r and when the value of N increases from 2, the fin's tip temperature become equal. We conclude that, in Figures 6(a) and 7(b), the temperature of fin's tip decreases for the growing value of N , due to heat drop from the surface through convection and radiation. Further, the effect of the surrounding temperature on the fin's tip is represented in Figure 7(c). This figure demonstrates that when the surrounding temperature rises along with the N , the temperature on the fin's tip increases rapidly. This increase is due to the decrease of convection from the fin to the surrounding.

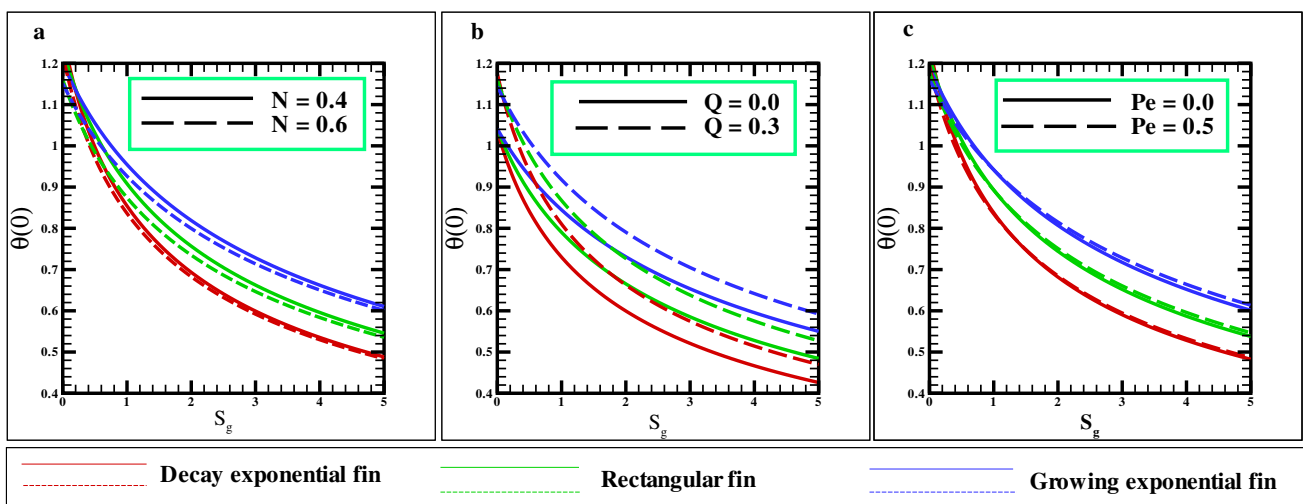


Figure 8. Comparison of fin's tip temperature for a variety of fins against the porosity parameter (a) The effects of convection-conduction number for $Pe = 0.2, Q = 0.2$. (b) The influence of internal heat generation for $N = 0.5, Pe = 0.2$ (c) The effects of Pe for $N = 0.5, Q = 0.2$. The other parameters are considered as $N_r = \theta_a = 0.2, \theta_s = 0.4$.

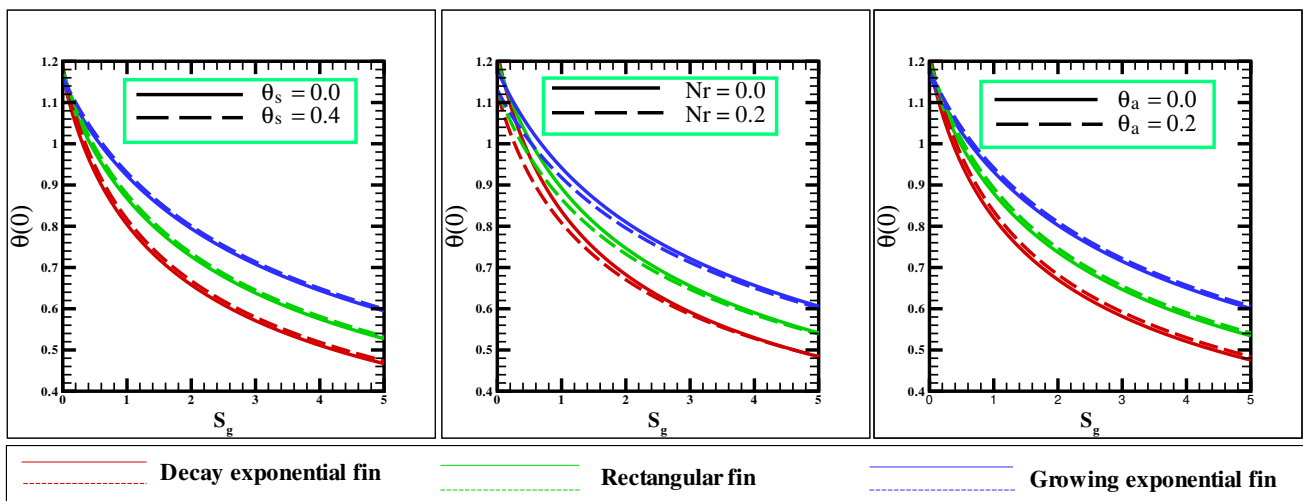


Figure 9. Comparison of fin's tip temperature for a variety of fins against the porosity parameter (a) The effects of surface temperature for $N_r = 0.2, \theta_a = 0.2$. (b) The effects of radiation conduction number for $\theta_a = 0.2, \theta_s = 0.4$. (c) The effects of ambient temperature for $N_r = 0.2, \theta_s = 0.4$. The other parameters are considered as $N = 0.5, Q = Pe = 0.2$.

In Figures 8 and 9, we study the connection of the temperature distribution of the fin's tip against porosity parameter S_g . The effect of convection-conduction number along with the porosity parameter on fin's tip temperature is represented in Figure 8(a). From this figure, one can see that, when N increases, the temperature on the fin's tip drop-down by increasing the value of porosity S_g . The effect of an internal heat generation is given in Figure 8(b). It should be noted that, for the minimum S_g , we obtain the maximum value of the tip temperature. The outcome of Pe on fin's tip temperature is shown in Figure 8(c). When the value of the Pe is increasing, the fin's tip temperature is increasing slightly.

In Figure 9(a), we note that the tip temperature grows as surface temperature increases. Similarly, Figure 9(b), shows that a small value of porosity parameter S_g , the fin's tip temperature decreases as we increase radiation-conduction number N_r and when the value of S_g increases, the fin's tip temperature come closer to each other. The result of the surrounding temperature on the tip of the fin is represented in Figure 9(c). This plot shows that as the surrounding temperature rises along with the porosity parameter, the temperature on the fin's tip increases slightly.

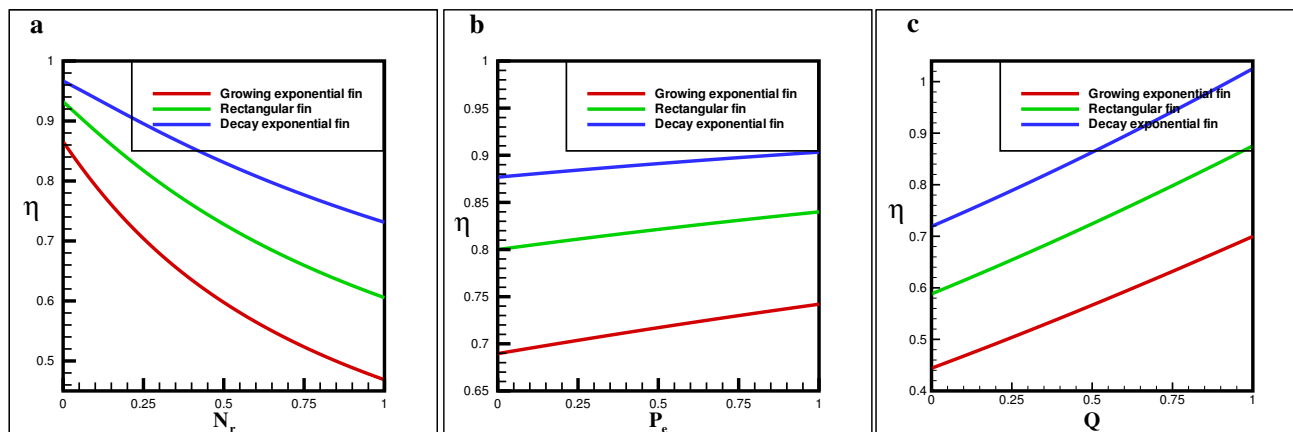


Figure 10. The plots represent the fin's efficiency against (a)The Radiation-conduction number N_r . (b)The Peclet Number Pe . (c)The heat generation Q . for the parameters are considered as $N_r = Q = Pe = \theta_a = 0.2$, $N = 0.5$, $\theta_s = 0.4$, $S_g = 0.2$.

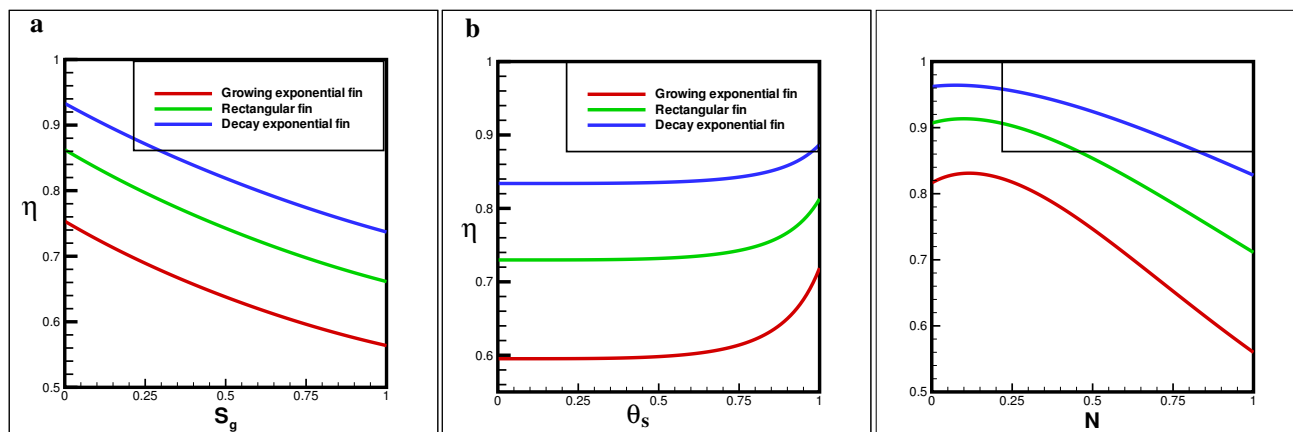


Figure 11. The plots represent the fin's efficiency against: (a)The porosity parameter. (b)The surface temperature. (c)The effect of convection-conduction number N . for the parameters are considered as $N_r = Q = Pe = \theta_a = 0.2$, $N = 0.5$, $\theta_s = 0.4$, $S_g = 0.2$.

In Figures 10 and 11, we demonstrate the influence of the radiation-conduction parameter N_r , Peclet number Pe and internal heat generation Q on the efficiency η together with the thermal conductivity parameter N_r , Pe , Q , S_g , θ_a , and θ_s for a variety of fins. From Figure 10(a), it is noted that, the fin efficiency is decreasing as N_r goes from 0 to 1. The impact of the Pe can be observed in Figure 10(b), which shows that the efficiency increases by increasing the Peclet number. From Figure 10(c), one can observe that fin's efficiency is decreasing for a large value of Q .

The influence of S_g on efficiency is expressed in Figure 11(a) shows that the fin's efficiency diminishes as the value of the porosity parameter increases. Figure 11(b) present that the fin's efficiency improve slightly as the surface temperature increases from $\theta_s = 0$ to $\theta_a = 0.75$ and increases rapidly as θ_s increases from 0.75. In Figure 11(c), we discuss the effect of convection-conduction number, which presents that increasing the value of N , the efficiency of the fin increases up to 0.25 and decreases as N rises from 0.25. In conclusion, it is observed that the efficiency of growing exponential fin is higher than a rectangular fin, while the efficiency of the rectangular fin is greater than a decay exponential fin as shown in Figures 10 and 11.

We conclude that the present work leads us to the conclusion that the straight fins frequently used in the industry can be replaced by the exponential fin of growing form to obtain a better convective heat exchange rate.

5. Conclusions

We have investigated the joint effect of convection, porosity and radiation on moving exponential fin under the influence of internal heat generation with convective boundary conditions. Three physically important parameters, efficiency, temperature distribution and fin's tip temperature are considered. It has been observed that the temperature distribution decreases by increasing heat generation, surrounding fluid's temperatures, the temperature of the fin surface, Peclet number, porosity parameter and increases by increasing convection-conduction and radiation-conduction number. It is also noticed that when the Peclet number increases, so do the local temperature, convection heat transfer, and surface heat loss, but the base heat conduction decreases. It is noted that the rectangular fins have lesser temperature distribution than exponential fins of decay exponential profile and greater value than growing exponential fins. When the surrounding temperature is increased by 50%, the efficiency of the fin decreases by approximately 30%. Increasing internal heat generation from 0.3 to 0.4 results in a 7% decrease in efficiency. The results demonstrate that the efficiency of the decay exponential fins is better than the fins of rectangular geometry. The existence of heat absorption supports the efficiency of the fin. Therefore, the fin's of the straight rectangular profile which is used widely in industries may be replaced with the decaying type of exponential for better performance as discussed in this article. It is possible to extend this research to analyze heat transfer from different fin types when a magnetic field is present. A single fin connected to the prime surface is the subject of this study. The research can incorporate an array of fins.

Acknowledgments

It is also declared that all the authors have equal contribution in the manuscript. Further, the authors have checked and approved the final version of the manuscript. Princess Nourah bint Abdulrahman University Researchers Supporting Project number (PNURSP2022R8). Princess Nourah bint Abdulrahman University, Riyadh, Saudi Arabia. The data regarding this manuscript is available within the manuscript.

Conflict of interest

It is declared that all authors have no conflict of interest regarding this manuscript.

References

1. M. Hatami, D. D. Ganji, M. Gorji-Bandpy, Experimental and numerical analysis of the optimized finned-tube heat exchanger for OM314 diesel exhaust exergy recovery, *Energy Convers. Manage.*, **97** (2014), 26–41. <https://doi.org/10.1016/j.enconman.2015.03.032>
2. M. Ghazikhani, M. Hatami, B. Safari, The effect of alcoholic fuel additives on exergy parameters and emissions in a two-stroke gasoline engine, *Arab. J. Sci. Eng.*, **39** (2014), 2117–2125. <https://doi.org/10.1007/s13369-013-0738-3>
3. M. Hatami, D. D. Ganji, Thermal performance of circular convective-radiative porous fins with different section shapes and materials, *Energy Convers. Manage.*, **76** (2013), 185–193. <https://doi.org/10.1016/j.enconman.2013.07.040>
4. M. Turkyilmazoglu, Heat transfer from moving exponential fins exposed to heat generation, *Int. J. Heat Mass Transfer*, **116** (2018), 346–351. <https://doi.org/10.1016/j.ijheatmasstransfer.2017.08.091>
5. E. Cuce, P. M. Cuce, Homotopy perturbation method for temperature distribution, fin efficiency and fin effectiveness of convective straight fins with temperature-dependent thermal conductivity, *J. Mech. Eng. Sci.*, **227** (2013), 1754–1760. <https://doi.org/10.1177/0954406212469579>
6. A. Y. Cengel, *Introduction to Thermodynamics and Heat Transfer*, Second Edition, McGraw-Hill Companies, 2008.
7. S. A. Atouei, K. Hosseinzadeh, M. Hatami, S. E. Ghasemid, S. A. R. Sahebi, D. D. Ganji, Heat transfer study on convective-radiative semi-spherical fins with temperature-dependent properties and heat generation using efficient computational methods, *Appl. Therm. Eng.*, **89** (2015), 299–305. <https://doi.org/10.1016/j.applthermaleng.2015.05.084>
8. K. Hosseinzadeh, E. Montazer, M. B. Shafii, A. R. D. Ganji, Solidification enhancement in triplex thermal energy storage system via triplets fins configuration and hybrid nanoparticles, *J. Energy Storage*, **34** (2021), 102177. <https://doi.org/10.1016/j.est.2020.102177>
9. M. Hatami, D. D. Ganji, Optimization of the longitudinal fins with different geometries for increasing the heat transfer, in *ISER 10th International Conference, Kuala Lumpur, Malaysia*, 2015.
10. M. Turkyilmazoglu, Heat transfer from moving exponential fins exposed to heat generation, *Int. J. Heat Mass Transfer*, **116** (2018), 346–351. <https://doi.org/10.1016/j.ijheatmasstransfer.2017.08.091>
11. B. Kundu, D. Bhanja, K. S. Lee, A model on the basis of analytics for computing maximum heat transfer in porous fins, *Int. J. Heat Mass Transfer*, **55** (2012), 7611–7622. <https://doi.org/10.1016/j.ijheatmasstransfer.2012.07.069>

12. Z. Din, A. Ali, S. Ullah, G. Zaman, Investigation of heat transfer from convective and radiative stretching/shrinking rectangular fins, *Math. Probl. Eng.*, **2022** (2022). <https://doi.org/10.1155/2022/1026698>
13. W. Ahmad, K. S. Syed, M. Ishaq, A. Hassan, Z. Iqbal, Numerical study of conjugate heat transfer in a double-pipe with exponential fins using DGFEM, *Appl. Therm. Eng.*, **111** (2017), 1184–1201. <https://doi.org/10.1016/j.applthermaleng.2016.09.171>
14. M. M. Rashidi, T. Hayat, T. Keimanesh, H. Yousefian, A study on heat transfer in a second-grade fluid through a porous medium with the modified differential transform method, *Heat Transfer Asian Res.*, **42** (2013), 31–45. <https://doi.org/10.1002/htj.21030>
15. E. Erfani, M. M. Rashidi, A. B. Parsa. The modified differential transform method for solving off-centered stagnation flow toward a rotating disc, *Int. J. Comput. Methods*, **7** (2010), 655–670. <https://doi.org/10.1142/S0219876210002404>
16. Y. Huang, X. Li, Exact and approximate solutions of convective-radiative fins with temperature-dependent thermal conductivity using integral equation method, *Int. J. Heat Mass Transfer*, **150** (2020), 119303. <https://doi.org/10.1016/j.ijheatmasstransfer.2019.119303>
17. M. M. Rashidi, E. Erfani, New analytical method for solving Burgers and nonlinear heat transfer equations and comparison with HAM, *Comput. Phys. Commun.*, **180** (2009), 1539–1544.
18. S. Panda, A. Bhowmik, R. Das, R. Repaka, S. C. Martha, Application of Homotopy analysis method and inverse solution of a rectangular wet fin, *Energy Convers. Manage.*, **80** (2014), 303–318. <https://doi.org/10.1016/j.cpc.2009.04.009>
19. R. K. Singla, R. Das, Application of decomposition method and inverse prediction of parameters in a moving fin, *Energy Convers. Manage.*, **84** (2014), 268–281. <https://doi.org/10.1016/j.enconman.2014.04.045>
20. C. Y. Zhang, X. F. Li, Temperature distribution of conductive-convective-radiative fins with temperature-dependent thermal conductivity, *Int. Comm. Heat Mass Transfer*, **117** (2020), 104799. <https://doi.org/10.1016/j.icheatmasstransfer.2020.104799>
21. S. W. Sun, X. F. Li, Exact solution of the nonlinear fin problem with exponentially temperature-dependent thermal conductivity and heat transfer coefficient, *Pramana J. Phys.*, **94** (2020), 1–10. <https://doi.org/10.1007/s12043-020-01971-4>
22. A. K. Asl, S. Hossainpour, M. M. Rashidi, M. A. Sheremet, Z. Yang, Comprehensive investigation of solid and porous fins influence on natural convection in an inclined rectangular enclosure, *Int. J. Heat Mass Transfer*, **133** (2019), 729–744. <https://doi.org/10.1016/j.ijheatmasstransfer.2018.12.156>
23. S. Maalej, A. Zayoud, I. Abdelaziz, I. Saad, M. C. Zaghoudi, Thermal performance of finned heat pipe system for Central Processing Unit cooling, *Energy Convers. Manage.*, **218** (2020), 112977. <https://doi.org/10.1016/j.enconman.2020.112977>
24. A. A. Joneidi, D. D. Ganji, M. Babaelahi, Differential Transformation Method to determine fin efficiency of convective straight fins with temperature dependent thermal conductivity, *Int. Commun. Heat Mass Transfer*, **36** (2009), 757–762. <https://doi.org/10.1016/j.icheatmasstransfer.2009.03.020>

25. C. H. Chiu, C. K. Chen, Applications of Adomian decomposition procedure to the analysis of convective radiative fins, *J. Heat Transfer*, **125** (2003), 312–316. <https://doi.org/10.1115/1.1532012>
26. D. Lesnic, P. J. Heggs, A decomposition method for power-law fin-type problems, *Int. Commun. Heat Mass Transfer*, **31** (2004), 673–682. [https://doi.org/10.1016/S0735-1933\(04\)00054-5](https://doi.org/10.1016/S0735-1933(04)00054-5)
27. R. Das, B. Kundu, Prediction of heat-generation and electromagnetic parameters from temperature response in porous fins, *J. Thermophys. Heat Transfer*, **35** (2021), 761–769. <https://doi.org/10.2514/1.T6224>
28. R. Das, B. Kundu, Simultaneous estimation of heat generation and magnetic field in a radial porous fin from surface temperature information, *Int. Commun. Heat Mass Transfer*, **127** (2021), 105497. <https://doi.org/10.1016/j.icheatmasstransfer.2021.105497>
29. D. Bhanja, B. Kundu, Thermal analysis of a constructal T-shaped porous fin with radiation effects, *Int. J. Refrig.*, **31** (2011), 337–352. <https://doi.org/10.1016/j.ijrefrig.2011.04.003>
30. B. Kundu, D. Bhanja, An analytical prediction for performance and optimum design analysis of porous fins, *Int. J. Refrig.*, **31** (2011), 1483–1496. <https://doi.org/10.1016/j.ijrefrig.2010.06.011>
31. R. Das, B. Kundu, Prediction of heat generation in a porous fin from surface temperature, *J. Thermophys. Heat Transfer*, **31** (2017), 781–790. <https://doi.org/10.2514/1.T5098>
32. R. Das, Forward and inverse solutions of a conductive, convective and radiative cylindrical porous fin, *Energy Convers. Manage.*, **87** (2014), 96–106. <https://doi.org/10.1016/j.enconman.2014.06.096>
33. R. Das, D. K. Prasad. Prediction of porosity and thermal diffusivity in a porous fin using differential evolution algorithm, *Swarm Evol. Comput.*, **23** (2015), 27–39. <https://doi.org/10.1016/j.swevo.2015.03.001>
34. B. Kundu, S. J. Yook, An accurate approach for thermal analysis of porous longitudinal, spine and radial fins with all nonlinearity effects-analytical and unified assessment, *Appl. Math. Comput.*, **402** (2021), 126124. <https://doi.org/10.1016/j.amc.2021.126124>
35. G. A. Oguntala, R. A. Abd-Alhameed, G. M. Sobamowo, N. Eya, Effects of particles deposition on thermal performance of a convective-radiative heat sink porous fin of an electronic component, *Therm. Sci. Eng. Prog.*, **6** (2018), 177–185. <https://doi.org/10.1016/j.tsep.2017.10.019>
36. M. A. Vatanparast, S. Hossainpour, A. Keyhani-Asl, S. Forouzi, Numerical investigation of total entropy generation in a rectangular channel with staggered semi-porous fins, *Int. Commun. Heat Mass Transfer*, **111** (2020), 104446. <https://doi.org/10.1016/j.icheatmasstransfer.2019.104446>
37. M. Turkyilmazoglu, Exact solutions to heat transfer in straight fins of varying exponential shape having temperature dependent properties, *Int. J. Therm. Sci.*, **55** (2012), 69–79. <https://doi.org/10.1016/j.ijthermalsci.2011.12.019>
38. Z. U. Din, A. Ali, G. Zaman, Entropy generation in moving exponential porous fins with natural convection, radiation and internal heat generation, *Arch. Appl. Mech.*, **92** (2022), 933–944. <https://doi.org/10.1007/s00419-021-02081-2>

39. Z. U. Din, A. Ali, M. D. la Sen, G. Zaman, Entropy generation from convective-radiative moving exponential porous fins with variable thermal conductivity and internal heat generations, *Sci. Rep.*, **12** (2022), 1791. <https://doi.org/10.1038/s41598-022-05507-1>
40. M. Hatami, A. Hasanpour, D. D. Ganji, Heat transfer study through porous fins (Si3N4 and AL) with temperature-dependent heat generation, *Energy Convers. Manage.*, **74** (2013), 9–16. <https://doi.org/10.1016/j.enconman.2013.04.034>
41. M. Hatami, D. D. Ganji, Thermal and flow analysis of microchannel heat sink (MCHS) cooled by Cu-water nanofluid using porous media approach and least square method, *Energy Convers. Manage.*, **78** (2014), 347–358. <https://doi.org/10.1016/j.enconman.2013.10.063>
42. M. Turkyilmazoglu, Thermal performance of optimum exponential fin profiles subjected to a temperature jump, *Int. J. Numer. Methods Heat Fluid Flow*, **32** (2021), 1002–1011. <https://doi.org/10.1108/HFF-02-2021-0132>
43. A. R. A. Khaled, Thermal characterizations of exponential fin systems, *Math. Probl. Eng.*, (2010), 765729. <https://doi.org/10.1155/2010/765729>
44. M. F. Najafabadi, H. T. Rostami, K. Hosseinzadeh, D. D. Ganji, Thermal analysis of a moving fin using the radial basis function approximation, *Heat Transfer*, **50** (2021), 7553–7567. <https://doi.org/10.1002/htj.22242>
45. S. Hosseinzadeh, K. Hosseinzadeh, A. Hasibi, D. D. Ganji, Thermal analysis of moving porous fin wetted by hybrid nanofluid with trapezoidal, concave parabolic and convex cross sections, *Case Stud. Therm. Eng.*, **30** (2022), 101757. <https://doi.org/10.1016/j.csite.2022.101757>
46. M. A. E. Moghaddam, M. R. H. S. Abandani, K. Hosseinzadeh, M. B. Shafii, D. D. Ganji, Metal foam and fin implementation into a triple concentric tube heat exchanger over melting evolution, *Theor. Appl. Mech. Lett.*, (2022), 100332. <https://doi.org/10.1016/j.taml.2022.100332>
47. B. Jalili, N. Aghaee, P. Jalili, D. D. Ganji, Novel usage of the curved rectangular fin on the heat transfer of a double-pipe heat exchanger with a nanofluid, *Case Stud. Therm.*, (2022), 102086. <https://doi.org/10.1016/j.csite.2022.102086>
48. B. Jalili, S. Sadighi, P. Jalili, D. D. Ganji, Characteristics of ferrofluid flow over a stretching sheet with suction and injection, *Case Stud. Therm.*, **14** (2019), 100470. <https://doi.org/10.1016/j.csite.2022.102086>
49. B. Jalili, S. Sadighi, P. Jalili, D. D. Ganji, Effect of magnetic and boundary parameters on flow characteristics analysis of micropolar ferrofluid through the shrinking sheet with effective thermal conductivity, *Chin. J. Phys.*, **71** (2021), 136–150. <https://doi.org/10.1016/j.cjph.2020.02.034>
50. P. Jalili, D. D. Ganji, B. Jalili, D. D. Ganji, Evaluation of electro-osmotic flow in a nanochannel via semi-analytical method, *Therm. Sci.*, **16** (2012), 1297–1302. <http://DOI:10.2298/TSCI1205297J>
51. M. Turkyilmazoglu, Efficiency of heat and mass transfer in fully wet porous fins: exponential fins versus straight fins, *Int. J. Refrig.*, **46** (2014), 158–164. <https://doi.org/10.1016/j.ijrefrig.2014.04.011>
52. B. Kundu, K. S. Lee, Analytic solution for heat transfer of wet fins on account of all nonlinearity effects, *Energy*, **41** (2012), 354–367. <https://doi.org/10.1016/j.energy.2012.03.004>

-
53. R. das, K. T. Ooi, Predicting multiple combination of parameters for designing a porous fin subjected to a given temperature requirement, *Energy Convers. Manage.*, **66** (2013), 211–219. <https://doi.org/10.1016/j.enconman.2012.10.019>
54. M. Torabi A. Aziz, K. Zhang, A comparative study of longitudinal fins of rectangular, trapezoidal and concave parabolic profiles with multiple nonlinearities, *Energies*, **51** (2013), 243–256. <https://doi.org/10.1016/j.energy.2012.11.052>



AIMS Press

©2022 the Author(s), licensee AIMS Press. This is an open access article distributed under the terms of the Creative Commons Attribution License (<http://creativecommons.org/licenses/by/4.0>)